Pergamon

Int. J. Solids Structures Vol. 34, No. 9, pp. 1035–1051, 1997

0020–7683/97 $17.00 + .00

PII: S0020–7683(96)00050–9

TIME DEPENDENT CRACKS IN CERAMIC MATRIX COMPOSITES: CRACK GROWTH INITIATION

M. R. BEGLEY*
The Division of Applied Science, Harvard University, Cambridge, MA 02138, U.S.A.

(*Received* 8 *November* 1995; *in revised form* 2 *April* 1996)

Abstract—Ceramic matrix composites at high temperatures exhibit time-dependent behavior due to fiber creep, even though the matrix remains elastic. The time-dependent behavior of bridged cracks for such materials is modeled using a bridging law developed previously which describes the effects of fibers bridging a matrix crack and accounts for frictional sliding between the fibers and the matrix. Approximations which simplify the bridging law are presented for short cracks or high loads. In particular, regimes are identified where the history-dependence of the crack opening rate can be neglected. Using a simplified form of the bridging law, results are presented for the general evolution of bridged stationary cracks. Determination of the bridging stress profile at a given instant in time allows calculation of the crack tip stress intensity factor as a function of time, leading to estimates for the time to initiate time-dependent crack growth. The results indicate that for very high loads and very short cracks, a simple form of bridging law can be used to produce accurate estimates for the initiation time to begin growing matrix cracks.

NOMENCLATURE

K_{tip}	stress intensity factor at the matrix crack tip
K_c	matrix toughness scaled for volume fraction (i.e., $K_c = (1-f)K_c^m$)
a, a_o	crack half-length and unbridged zone half-length
τ	shear sliding stress between the fibers and matrix
D	diameter of the fibers
f	fiber volume fraction
E_f, E_m	Young's modulus of the fibers and the matrix,
$E_L = fE_f + (1-f)E_m$	rule of mixtures Young's modulus for the composite
$\bar{E}$	Young's modulus which accounts for orthotropy
$\lambda = \frac{D(1-f)^2E_m^2}{4\tau f^2 E_f E_L^2}$	rate-independent bridging law coefficient
$\eta = \frac{fE_f - (1-f)E_m}{E_L}$	coefficient used in the rate-dependent bridging law
$C(\sigma, t, T)$	convolution integral used in the bridging law
B	creep coefficient of the fibers
$\beta = BE_f$	modified creep coefficient
$T = \frac{E_L}{(1-f)BE_mE_f}$	characteristic relaxation time for the intact composite
$\bar{\beta} = \frac{BE_fE_L}{2(1-f)E_m}$	modified creep coefficient for the simplified bridging law
$\delta, \dot{\delta}$	total crack opening and opening rate
$\sigma, \dot{\sigma}$	bridging traction and traction rate
σ_a	applied load
$\Sigma = \frac{\lambda\bar{E}\sigma}{a}$	normalized bridging traction
$\Sigma_a = \frac{\lambda\bar{E}\sigma_a}{a}$	normalized applied load
$\kappa = \frac{K_{tip}}{\sigma_a\sqrt{\pi a}}$	normalized stress intensity factor at the matrix crack tip.

*Formerly at the Mechanical and Environmental Engineering Department, College of Engineering, University of California, Santa Barbara, Santa Barbara, California 93106, U.S.A.

1. INTRODUCTION

Ceramic matrix composites reinforced with long ceramic fibers exhibit a variety of creep modes at high temperatures (Evans and Zok, 1994; Holmes and Chermand, 1993). The mode in which fibers creep and the matrix is elastic has often been identified as the most critical. Fiber creep sheds loads to the matrix, increasing the likelihood of matrix cracking. Also, bridged crack growth is possible even under constant load, as creeping fibers will provide bridging tractions which decay with time (Henager and Jones, 1993, 1994; Begley *et al.*, 1995). Since bridged cracks geometries are often considered to be unavoidable, the time-dependent behavior of bridged cracks is of central interest.

Predicting the time dependent high temperature behavior of bridged cracks in CMCs can be thought to have two primary components: i) predicting the time it takes to initiate rate-dependent crack growth and ii) predicting crack growth evolution and fiber failure in order to determine rupture times. Clearly the magnitudes of these times will govern the relative importance of each component; if time to initiate crack growth is long and the ensuing crack growth is rapid, the initiation time will be of more significance. Conversely, if crack growth starts rapidly after exposing the material to creep temperatures but growth rates are slow, initiation times are not as important as determining relevant crack growth rates. Relevant crack growth studies have been performed previously (Begley *et al.*, 1995; Begley *et al.*, 1995a, 1995b). Initiation times for bridged cracks in CMCs are presented here.

In order for initiation times to be pertinent, a bridged crack geometry must exist in which the stress intensity at the matrix crack tip, K_{tip}, is lower than the matrix toughness adjusted for the matrix volume fraction, denoted K_c. The initiation time to crack growth is then the amount of time it takes to degrade the bridging tractions sufficiently to raise the crack tip stress intensity factor to K_c. (If the bridged geometry is created under the condition $K_{tip} = K_a$, such as the case considered in [Begley *et al.*, 1995a], the initiation time will be zero.) There are two primary scenarios in which bridged cracks are created such that $K_{tip} < K_c$.

The first scenario where $K_{tip} < K_c$ (for bridged cracks) results from processing flaws that may exist in the material. Composites with SiC fibers, which are of primary interest in these applications, are particularly susceptible to large flaws (Bourrat *et al.*, 1995). For many cases, a processing flaw which spans multiple fibers and is perpendicular to the loading direction can be thought of as an unloaded bridged crack. For a flaw with no remote loading, $K_{tip} = 0$. As the load is increased, the bridged crack opens monotonically and K_{tip} rises. At fixed load (provided $K_{tip} < K_c$), some finite time is required to relax the bridging tractions via creep so that K_{tip} grows to K_c and crack growth occurs.

A second possibility for bridged cracks where $K_{tip} < K_c$ is the case of an over-load. Consider a bridged crack grown under the condition $K_{tip} = K_c$; the crack length will increase as the load is increased. When the load is decreased, the crack length will remain at the length reached at the maximum load, but K_{tip} will decrease as the applied load decreases and bridging becomes more effective (McMeeking and Evans, 1990). With sufficient unloading, the condition $K_{tip} < K_c$ will be reached.

The case of a bridged crack where $K_{tip} < K_c$ is not a simple one when unloading occurs. Upon unloading, the nature of the bridging law governing the bridging traction profile changes, resulting in a "reverse slip zone" where the direction of shear stress between the fiber and matrix changes (McMeeking and Evans, 1990). With no creep present, the influence of these reverse slip zones on the bridging law and bridged crack behavior is straightforward and well understood (McMeeking and Evans, 1990; Bao and McMeeking, 1994). Creep complicates the situation and, as of yet, a complete time-dependent bridging law which incorporates reverse slip is not yet available. A bridging law derived for the case of "forward slip" will still capture the time dependent nature of the problem, however; as such one will be used in this work. The effect of this approximation will be discussed further in Section 6.

Neglecting the possibility of reverse slip, the problem of cracks created from an overload is identical to the case where processing flaws are considered to be cracks. The

initial condition for both cases is taken to be the rate-independent solution for a bridged crack under a constant applied load.

Initiation times are relevant for these scenarios provided the load is large enough to grow an unbridged crack in the matrix. Fiber creep will eventually completely relax the bridging tractions supplied by the fibers, resulting in an unbridged crack in an elastic material. The applied load must be high enough to propagate this unbridged flaw. Additionally, the load must be below the matrix cracking stress of the composite to prevent catastrophic rate-independent cracking [e.g., Marshall *et al.*, 1985; McCartney, 1987; Cox and Marshall, 1991].

While initiation times in other materials have been investigated (Schapery, 1975; Nair *et al.*, 1991; Knauss, 1993), there has been only two analyses of initiation times for CMCs. The work of Nair *et al.* (1991) considered initiation times for CMCs with a time-dependent interface between the fibers and matrix. Since many CMCs have interfaces which do not creep, the analysis presented here for frictional slip is more appropriate. El-Azab and Ghoniem have considered the problem of bridged cracks with creeping fibers in an elastic matrix with frictional slip (El-Azab and Ghoniem, 1994); the method presented here is meant as an alternative approach to the problem which is more easily connected with previous rate-independent analyses. Additionally, results are presented for partially bridged matrix cracks, which are relevant to machined notches and flaws with regions which have no fibers.

The formulation presented here is easily recognizable in terms of previous bridged crack models for fiber-reinforced composites (Marshall *et al.*, 1985; McCartney, 1987; McMeeking and Evans, 1990; Cox and Marshall, 1991; Bao and McMeeking, 1994; Begley and McMeeking, 1995; Begley *et al.*, 1995, 1995a, 1995b). The use of a bridging law based on a cell model allows for convenient extension of the line-spring models developed for rate-independent behavior. As such, the method and results described in this work for time-dependent phenomena can be connected to previous analyses presented for rate-independent behavior. This is important when considering transitions from stationary cracks to subcritical or catastrophic crack growth.

Results are presented here for a center crack of length $2a$ in a panel of infinite width. The loading is remote tension, as shown in Figure 1. The model is relevant to unidirectional composites and laminates with an appropriate orientation, as outlined in Begley *et al.*, 1995a. For the approximations considered in Section 2, the crack is considered to be fully bridged, while this restriction is relaxed for the general analyses outlined in Section 4.

1.1. *The general time dependent bridging law*

The derivation of the time-dependent bridging law was outlined in the work of Begley *et al.* (1995). The law was derived using a cell model similar to the elastic case; the fibers are assumed to creep linearly and the matrix is elastic; frictional sliding occurs between the fibers and the matrix and is resisted by a time-independent shear stress τ. Residual stresses are ignored as they usually relax via creep. The result is

$$\dot{\delta}(x,t) = \lambda\left\{\sigma(x,t)+f\beta\frac{E_f}{E_L}C(\sigma,t,T)\right\}\left[2\dot{\sigma}(x,t)+2\beta\sigma(x,t)+\beta\eta\left(\sigma(x,t)+f\beta\frac{E_f}{E_L}C(\sigma,t,T)\right)\right] \tag{1}$$

where σ and $\dot{\sigma}$ are the bridging traction and traction rate, respectively; λ is the same bridging coefficient as the elastic case (where $\delta = \lambda\sigma^2$ [McCartney, 1987; Hutchinson and Jensen, 1990]) and is given by

$$\lambda = \frac{D(1-f)E_m^2}{4f^2\tau E_L^2 E_f}. \tag{2}$$

D is the fiber diameter; f is the fiber volume fraction; E_f, E_m and $E_L = fE_f+(1-f)E_m$ are

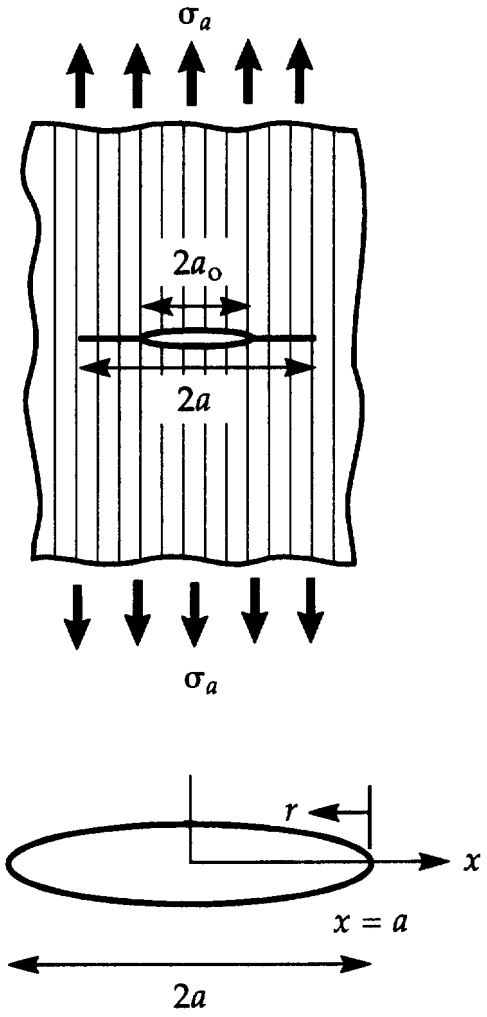

Fig. 1. Bridged crack geometry and coordinate systems.

the fiber, matrix and composite elastic moduli, respectively. η is a non-dimensional function of the elastic moduli, given by

$$\eta = \frac{fE_f - (1-f)E_m}{E_L}. \tag{3}$$

The history dependence of the problem is contained in the convolution integrals, C, given as

$$C(\sigma, t, T) = \int_{-\infty}^{t} \sigma(x, \bar{t}) e^{-(t-\bar{t})/T} \, \mathrm{d}\bar{t} \tag{4}$$

where

$$T = \frac{E_L}{(1-f)BE_mE_f} = \frac{E_L}{E_m} \frac{1}{\beta(1-f)} \tag{5}$$

is the characteristic relaxation time for the intact composite (McLean, 1985). B is the creep coefficient of the fibers (from the creep law for the fibers, i.e. $\dot{\varepsilon} = \dot{\delta}/E + B\sigma$), and

$$\beta = BE_f \tag{6}$$

is a modified creep coefficient with the dimension t^{-1}. Creep data for Nicalon (SiC) fibers can be found in (DiCarlo and Morscher, 1991; Tressler and DiCarlo, 1993).

1.2. *A simplified bridging law for time-dependent bridging in an elastic bulk material*

For times much smaller than the characteristic time of the intact composite (i.e., $t \ll T$), the convolution integrals in (1) can be neglected. With neglect of the convolution integrals, the bridging law simplifies to†

$$\dot{\delta}(x,t) = 2\lambda\sigma(x,t)[\dot{\sigma}(x,t) + \bar{\beta}\sigma(x,t)], \tag{7}$$

where

$$\bar{\beta} = \beta\left(1+\frac{\eta}{2}\right) = BE_f\left(\frac{1}{2}+\frac{fE_f}{E_L}\right). \tag{8}$$

This approximation is the same as assuming the bulk material surrounding the crack is elastic (Begley *et al.*, 1995a). Creep then only occurs in the slip zones—small regions adjacent to the crack plane. The slip length behavior is simplified from that of the full bridging law, in that the slip lengths will be fixed at constant bridging stress. (As the bridging stress decreases via creep, however, the slip lengths will increase). Making this simplification greatly reduces the complexity of the problem, as the history dependence of the bridging law is removed. That is, the crack opening rate will not be dependent on all previous values of the bridging stress (and stress rate), merely on the instantaneous values at a given time. The simplicity of this law makes this an attractive form of the bridging law, and it is used in Section 4 for full integral equation solutions of bridging traction profiles.

2. APPROXIMATIONS BASED ON PARABOLIC PROFILES

2.1. *Derivation of the governing differential equation*

Insight into the time-dependent behavior of bridged cracks can be gained by considering a simple approximation for the spatial dependence of bridging stress for a fully bridged crack. For very short cracks, or cracks under high loads, the bridging stress profile is approximated as a separable function in time and space, as in

$$\sigma(x,t) \approx \sigma_o(t)[1-\bar{x}^2]^{1/4} \tag{9}$$

where $\bar{x} = x/a$ and a is the crack half length.

This profile was chosen because it is asymptotically correct at high loads, where the bridging traction does not significantly alter the spatial dependence of the crack opening profile from that of an unbridged crack. Additionally, the rate-independent behavior of this approximation has been considered previously and provides the basis for determining when such a profile is applicable (Marshall *et al.*, 1985). This approximation is compared with complete numerical results in Section 5.

By explicitly imposing the spatial dependence of the bridging traction, the profile evolves over time with a self-similar profile. The magnitude of the bridging traction distribution is given by $\sigma_o(t)$ and this is assumed to completely capture the time dependence of the problem. Thus, the time derivative of the bridging traction distribution is

$$\dot{\sigma}(x,t) = \dot{\sigma}_o(t)[1-\bar{x}^2]^{1/4}. \tag{10}$$

The near tip crack opening profile can be expressed as (Tada *et al.*, 1985)

† A form identical to this was used in Begley *et al.*, 1995a. The modified creep coefficient is different, however, as the form previously derived neglects different terms. A simple substitution of the desired form of β is possible; hence, the difference does not affect the results.

$$\delta(r,t) = \frac{8K_{tip}(t)}{\bar{E}}\sqrt{\frac{r}{2\pi}} \tag{11}$$

where r is measured from the matrix crack tip (see Figure 1). K_{tip} is the crack tip stress intensity factor and $\bar{E}$ is a composite elastic modulus which accounts for orthotropy (Bao and McMeeking, 1994). The stress intensity factor at the crack tip can be expressed in terms of an integral of the bridging traction distribution via standard elastic fracture mechanics (Tada *et al.*, 1985). Using (9) to express the spatial dependence of the bridging stress, this equation for the near tip crack opening profile results:

$$\delta(r,t) = \frac{2\sqrt{ra}}{\sqrt{2}\bar{E}}\left[\sigma_a - \frac{4(1.2)}{\pi}\sigma_o(t)\right]. \tag{12}$$

The first term is the crack opening due to the applied load σ_a, while the second term is the crack closure due to the bridging tractions. Here, it has been assumed that the crack opening due to the applied load is constant in time; i.e., creep in the bulk material surrounding the crack has been neglected.†

Differentiation with respect to time of (12) yields the crack opening rate in terms of the bridging traction rate

$$\dot{\delta}(r,t) = -\frac{16(1.2)}{\sqrt{2}}\frac{\sqrt{ra}}{\pi\bar{E}}\dot{\sigma}_o(t). \tag{13}$$

The bridging law given as (1) provides a second expression for the crack opening rate. Using (9) and (10) to represent the spatial dependence of the bridging stress and stress rate, respectively, the bridging law becomes

$$\dot{\delta}(x,t) = \lambda[1-\bar{x}^2]^{1/2}\left\{\sigma_o(t)+f\beta\frac{E_f}{E_L}C\right\}\left[2\dot{\sigma}_o(t)+2\beta\sigma_o(t)+\beta\eta\left(\sigma_o(t)+f\beta\frac{E_f}{E_l}C\right)\right]. \tag{14}$$

Note that $x = r-a$; using this relation, the spatial dependence in front of (14) can be approximated near the crack tip as $\sqrt{2r/a}$. Equating (13) and the bridging law results in the following differential equation for the magnitude of the bridging stress profile:

$$\frac{8(1.2)}{\pi}\frac{a\dot{\sigma}_o(t)}{\bar{E}} = \lambda\left\{\sigma_o(t)+f\beta\frac{E_f}{E_L}C\right\}\left[2\dot{\sigma}_o(t)+2\beta\sigma_o(t)+\beta\eta\left(\sigma_o(t)+f\beta\frac{E_f}{E_L}C\right)\right]. \tag{15}$$

Equation (15) can be normalized by multiplying by $\lambda\bar{E}^2/a^2$; upon rearrangement, this gives

$$\dot{\Sigma} = -\frac{\left[\left\{\Sigma+f\beta\frac{E_f}{E_L}C\right\}\left[2\beta\Sigma+\beta\eta\left(\Sigma+f\beta\frac{E_f}{E_L}C\right)\right]\right]}{\left[\frac{8(1.2)}{\pi}+2\Sigma+2f\beta\frac{E_f}{E_L}C\right]} \tag{16}$$

where $\Sigma = (\lambda\bar{E}\sigma_o(t)/a)$. Note that the convolution integrals given by (4) have become functions of $\Sigma(t)$ rather than $\sigma_o(t)$; i.e., $C = C(\Sigma, t, T)$. Equation (16) represents the full differential equation which governs the behavior of the bridging traction profile.

† This assumption is not completely necessary; calculations are being done for a bridged stationary crack in a linearly viscoelastic bulk material.

2.2. *Initial conditions for the bridging stress magnitude*

The initial value of the bridging stress magnitude, $\Sigma(0)$ is found by equating (12) to the rate-independent bridging law, given by McCartney, 1985; Hutchinson and Jensen, 1990

$$\delta(r, 0) = \lambda[\sigma(r, 0)]^2. \tag{17}$$

The result is a quadratic expression for the initial magnitude of the bridging stress profile in terms of the applied load. After appropriate normalization, the initial condition is given by

$$\Sigma(0) = \sqrt{\left(\frac{4.8}{\pi}\right)^2 + 4\Sigma_a} - \frac{4.8}{\pi}. \tag{18}$$

where $\Sigma_a = \lambda \bar{E}\sigma_a/a$.

The solution for the bridging stress evolution in time is then obtained by solving the differential eqn (16) using standard numerical techniques (e.g., the forward Euler method), where the initial value is given by (18).

2.3. *Simplifications of the governing differential equation*

Equation (16) can be simplified by considering realistic values of the composite properties; taking $f = 1/3$ and $E_f = E_m = E_L$, the following expression results after some algebraic manipulation;

$$\dot{\Sigma} = -\frac{\beta\left[\frac{5}{3}\Sigma^2 + \frac{4}{9}\Sigma\bar{C} - \frac{1}{27}\bar{C}^2\right]}{\left[\frac{9.6}{\pi} + 2\Sigma + \frac{2}{3}\bar{C}\right]} \tag{19a}$$

where

$$\bar{C} = \int_{-\infty}^{\beta t} \Sigma(\beta\bar{t}) e^{-2\beta(t-\bar{t})/3T}\, d\bar{t}. \tag{19b}$$

Note that time appears only in the product βt; the solution can therefore be determined without specifying β directly, as it will appear in the normalized time βt.

Furthermore, considering times much smaller than T allows neglect of the convolution integrals;

$$\dot{\Sigma} = -\frac{\left[\frac{5}{3}\beta\Sigma^2\right]}{\left[\frac{9.6}{\pi} + 2\Sigma\right]}. \tag{20}$$

The differential eqns (19) and (20) were solved numerically and used to compare the effect

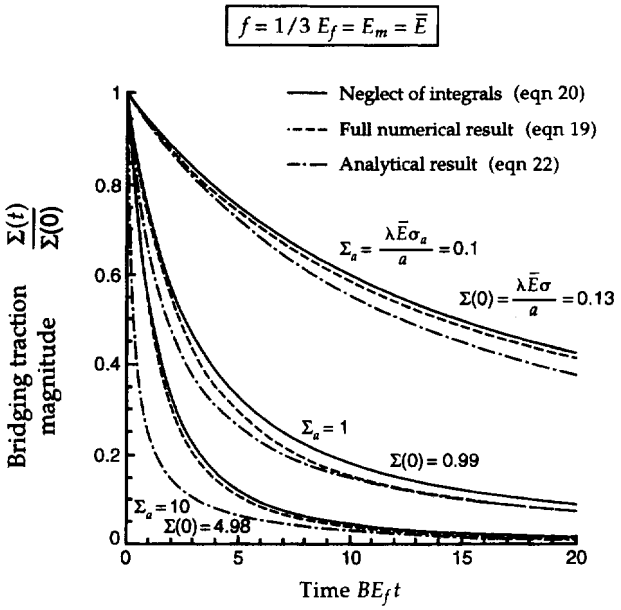

Fig. 2. Bridging stress magnitude as a function of time for the parabolic approximation.

of neglecting the convolution integrals. The results are shown in Fig. 2, depicting the bridging stress magnitude as a function of time.

Lastly, for very small Σ_a, the bridging stress magnitude in the denominator can be neglected, leading to

$$\dot{\Sigma} = -\frac{5\pi}{28.8}\beta\Sigma^2. \tag{21}$$

The last simplification is probably not realistic, as small Σ_a corresponds to large crack lengths or small applied loads, in which case the assumed spatial dependence in (10) is not accurate. However, this allows an analytical solution which can be quickly compared to the numerical solutions of (19) and (20). The analytical solution of (21) is given by

$$\Sigma(t) = \frac{\Sigma(0)}{1+\Sigma(0)\dfrac{5\pi}{28.8}\beta t}. \tag{22}$$

The result is plotted in Fig. 2 along with the numerical solutions to (19) and (20).

2.4. *Crack tip stress intensity factors*

Once the bridging stress profile is obtained, the crack tip stress intensity factor for each instant in time can be calculated in a straightforward manner (Tada *et al.*, 1985);

$$K_{tip}(t) = \sigma_a\sqrt{\pi a} - \frac{2\sqrt{a}}{\sqrt{\pi}}\int_0^1 \frac{\sigma_o(t)\,d\bar{x}}{(1-\bar{x}^2)^{1/4}}. \tag{23}$$

Using the normalization presented earlier and performing quadrature, the non-dimensional form of K_{tip} is found to be

$$\kappa(t) = \frac{K_{tip}(t)}{\sigma_a\sqrt{\pi a}} = 1 - \frac{2.4}{\pi}\frac{\Sigma(t)}{\Sigma_a}. \tag{24}$$

The solutions of eqns (19), (20) and (21) can be used with this expression to predict the

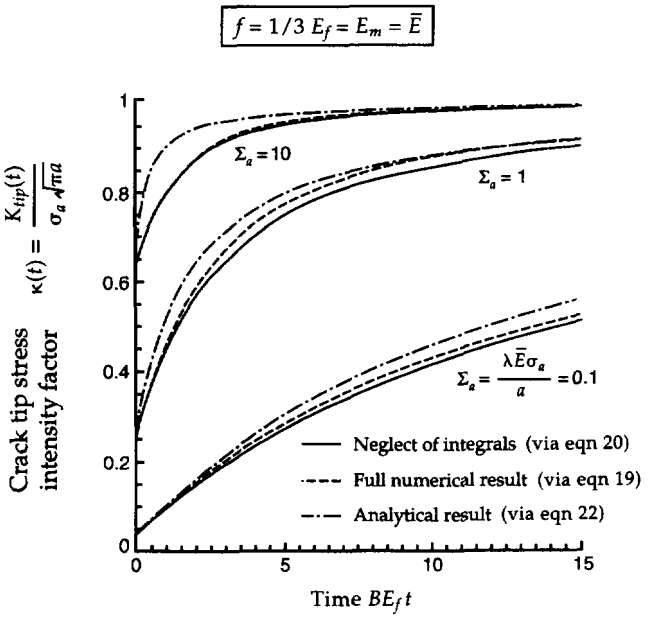

Fig. 3. Crack tip stress intensity factors as a function of time using the results of the parabolic approximation.

stress intensity factor of the matrix crack tip as a function of time. Figure 3 shows $\kappa(t)$ using the results of eqns (19), (20) and (22).

3. EFFECT OF SIMPLIFYING THE BRIDGING LAW ON PARABOLIC APPROXIMATION RESULTS

The effect of simplifying the bridging law can be determined by examining the results shown in Figs 2 and 3. As expected, all results show a sharp drop in the bridging stress over a short time, with a decreasing rate of decay. For higher loads, the bridging stress drops more quickly, as higher loads (and therefore higher bridging tractions) drive higher creep rates. The results for the bridging traction profiles affect the crack tip stress intensity factor as one would expect; higher loads and faster decay cause the crack tip stress intensity factor to rise quickly and approach the case of an unbridged crack. It should be noted that the results in Fig. 3 reflect the decrease in bridging effectiveness as load is increased; the curves for higher loads start at greater κ, as shielding is less pronounced.

For times smaller than $1/\beta$, the approximations to the full equation work fairly well. (This is on the order of one hour for a SiC/SiC material at 1100°C.) As time increases, the approximation show increasing error due to the neglect of the convolution integrals given as (19b). Neglect of the bridging stress term in the denominator in (20) is appropriate at lower loads but improper at realistic values of normalized load. Indeed, this approximation does not seem worthwhile, as it appears to be good only for the lowest load case. The question of interest is whether or not the convolutions in (19) can be neglected.

For short times, the convolution integrals (19) do not significantly contribute to the time-dependent bridging behavior. As time is increased, they become more significant with increasingly growing error. This is particularly true for low loads. It is appropriate to mention that the results for the parabolic approximation are probably not very accurate at small loads due to inconsistency between the imposed and actual crack opening profile. At high loads, the error introduced by neglecting the convolutions is negligible.

4. PROBLEM FORMULATION FOR THE GENERAL SOLUTION OF BRIDGED STATIONARY CRACKS

4.1. *Derivation of the governing integral equation*

The bridging stress distribution can be solved for exactly (without any assumptions about spatial dependence) by formulating an integral equation for the time derivative of

the traction distribution. The derivation follows the same procedure as most bridging problems; the crack opening relation from fracture mechanics is equated to the appropriate bridging law.

In general, the total crack opening profile for a partially bridged center crack in an infinite body can be written as (Tada *et al.*, 1985)

$$\delta(x,t) = \delta_a(x,t) - \frac{4}{\pi\bar{E}}\int_{a_o}^{a}\sigma(\bar{x},t)\ln\left|\frac{\sqrt{a^2-\bar{x}^2}+\sqrt{a^2-x^2}}{\sqrt{a^2-\bar{x}^2}-\sqrt{a^2-x^2}}\right|d\bar{x} \tag{25}$$

where $\delta_a(x,t)$ is the crack opening due to the applied load, $\sigma(x,t)$ is the bridging traction and a_o is the half length of the unbridged region (or notch). The second term represents the decrease in opening due to the bridging traction supplied by the fibers.

Since the applied loads considered here are constant and the bulk material surrounding the crack is considered to be elastic, the crack opening due to applied load will be constant with respect to time. Differentiating (25) with respect to time and equating the result to the simplified bridging law (given as (7)) yields the following integral equation for the bridging traction rate profile:

$$\frac{4}{\pi\bar{E}}\int_{a_o}^{a}\dot{\sigma}(\bar{x},t)\ln\left|\frac{\sqrt{a^2-\bar{x}^2}+\sqrt{a^2-x^2}}{\sqrt{a^2-\bar{x}^2}-\sqrt{a^2-x^2}}\right|d\bar{x}+2\lambda\sigma(x,t)\dot{\sigma}(x,t) = -2\lambda\bar{\beta}[\sigma(x,t)]^2 \tag{26}$$

where $\dot{\sigma}(x,t)$ is the time derivative of the bridging traction profile. This equation can be normalized by multiplying both sides by $\lambda\bar{E}^2/a^2$, resulting in dimensionless form of the governing equation;

$$2\int_{\alpha}^{1}\dot{\Sigma}(\bar{x},t)H(\bar{x},x,1)\,d\bar{x}+\dot{\Sigma}(x,t)\Sigma(x,t) = -\bar{\beta}[\Sigma(x,t)]^2 \tag{27}$$

where $\alpha = a_o/a$ is the normalized notch size, the normalized bridging traction is given by $\Sigma = \lambda\bar{E}\sigma/a$, and H is a weight function given by

$$H(\bar{x},x,1) = \frac{1}{\pi}\ln\left|\frac{\sqrt{1-\bar{x}^2}+\sqrt{1-x^2}}{\sqrt{1-\bar{x}^2}-\sqrt{1-x^2}}\right|. \tag{28}$$

Note that the spatial location x and dummy integration variable $\bar{x}$ have been normalized by the crack length a, rendering them dimensionless.

4.2. *Numerical solution of the problem and the initial conditions*

The solution of (27) gives the rate of change in the bridging traction profile for a given time t when the bridging traction profile is known. Since the bridging stress distribution at time zero is taken as the rate-independent response, the method is self starting in that all the quantities needed to calculate the time derivatives at time zero are known; as such, standard methods can be used to solve the differential equation given as (27). The problem is an iterative one, where the bridging stress rate is determined via (27) for a given time and used to predict the bridging stress at the next time step. The procedure is summarized in the Appendix.

4.3. *Determining the crack tip stress intensity factor*

Once the bridging stress is determined for a given time, the instantaneous values of the stress intensity factor at the matrix crack tip, K_{tip}, can be calculated by integrating the effect of the bridging stress, as was done in Section 2.4 using eqn (23). For this case however, the spatial dependence of the bridging traction profile cannot be removed (Tada *et al.*, 1985);

$$\kappa(t) = \frac{K_{tip}(t)}{\sigma_a\sqrt{\pi a}} = 1 - \frac{2}{\pi\Sigma_a}\int_\alpha^1 \frac{\Sigma(\bar{x}, t)\,d\bar{x}}{\sqrt{1-\bar{x}^2}}. \tag{29}$$

The discretized values of the bridging traction are used to evaluate the second term. Note that as time elapses, the relaxation of the bridging tractions will eliminate the effects of bridging, and the stress intensity factor at the crack tip will approach that of an unbridged crack.

5. RESULTS

5.1. *Bridging traction profile evolution*

Bridging traction profiles are shown for several time steps in Fig. 4(a–c) for a fully bridged crack subjected to three applied loads. The figures reveal that the bridging traction will rapidly decay as creep relaxes the fibers. At higher loads, the loss of crack tip shielding is much more rapid. For the fully bridged case, the profiles evolve over time with nearly a self-similar profile; indeed, at higher loads the profile is nearly perfectly matched with the approximation in Section 2 (given by (9)).

The effect of an unbridged region of matrix crack (or notch) is illustrated in Fig. 5(a–c). The interesting thing to note is that the bridging tractions at the notch relax away fairly rapidly; the curves shown in Fig. 5(a) show that the stress concentration of the notch is completely relaxed by the time $\beta t = 2.5$. The reason for the more rapid decay of the traction at the notch is obvious; the stress at the notch is high and therefore the fibers creep very quickly. The time histories of the bridging traction at the center of the crack (for the fully bridged case) and at the notch are shown in Fig. 6. These figures emphasize the rapid decrease in bridging tractions at these locations when loads are high.

5.2. *Crack tip stress intensity factor as a function of time*

The traction profiles (such as those plotted in Fig. 4(a–c) and 5(a–c)) were used in conjunction with eqn (29) to predict the crack tip stress intensity factor as a function of time. The results for three notch sizes and three loads are shown in Fig. 7. As time progresses, the bridging tractions decay via creep relaxation and K_{tip} rises. Eventually, creep completely relaxes the bridging tractions, indicating shielding has disappeared and K_{tip} equals the applied value. The time to crack growth initiation can be determined merely by computing $K_a = \sigma_a\sqrt{\pi a}$ for a given load and flaw size and finding the time where $K_{tip} = K_c$ on the appropriate curve in Fig. 7.

5.3. *Comparison of full distribution results and assumed profile results*

For fully bridged cracks, the parabolic approximation of Section 2 can be directly evaluated by comparing the results with the more detailed calculations of Section 4. The bridging stress magnitudes as the center of the crack are compared in Fig. 8. The crack tip stress intensity factors for the same cases are shown in Fig. 9.

At high loads, the parabolic profile works quite well. Both the curves for the bridging stress magnitude and the crack tip intensity factor are similar. The agreement between the parabolic results and the general results at high loads can be quite striking, as the bridging traction profiles are indeed nearly completely captured by eqn (9). The agreement between the two cases for these higher loads clearly indicates the solutions presented in Section 2 are quite acceptable for predicting crack growth initiation times for such cases.

For lower loads or larger crack lengths, however, the results may be quite different; note the difference in Σ at time zero in Fig. 8. The differences in the crack stress intensity factor for these cases can be traced to the error in bridging traction magnitude due to the incorrect assumed profile. Recall that the approximations in Section 2 were based on matching the near tip behavior with asymptotic solutions; subsequently, bridging tractions farther from the crack tip may have significant error.

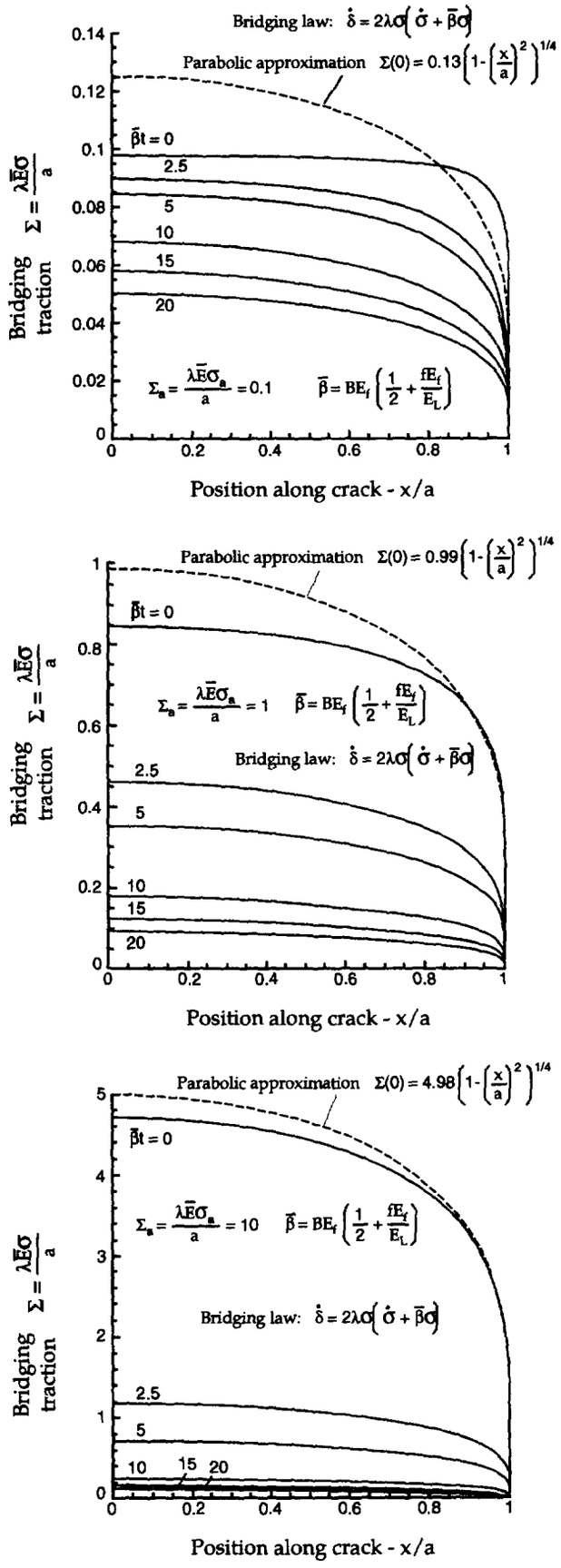

Fig. 4. Bridging stress profiles at $\beta t = 0$, 2.5, 5, 10, 15, 20 for the fully bridged case; (a) $\Sigma_a = 0.1$ (b) $\Sigma_a = 1$ (c) $\Sigma_a = 10$.

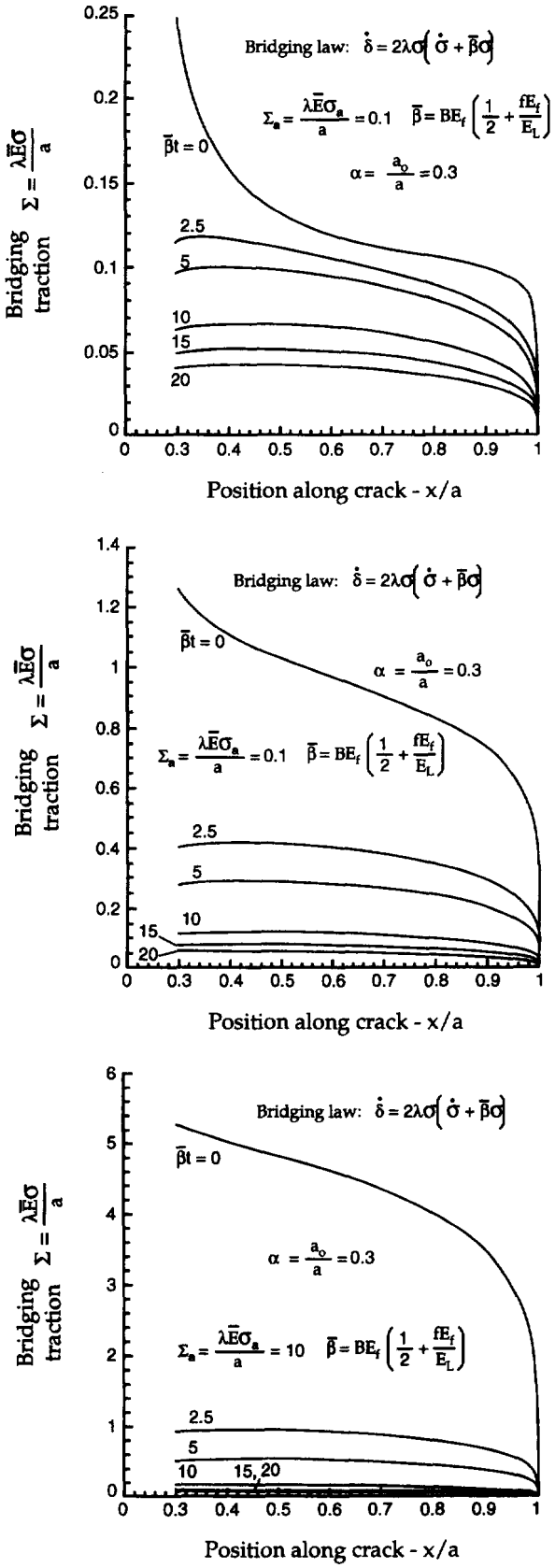

Fig. 5. Bridging stress profiles at $\beta t = 0, 2.5, 5, 10, 15, 20$ for a partially bridged crack; (a) $\Sigma_a = 0.1$, $\alpha = 0.3$ (b) $\Sigma_a = 1$, $\alpha = 0.3$ (c) $\Sigma_a = 10$, $\alpha = 0.3$.

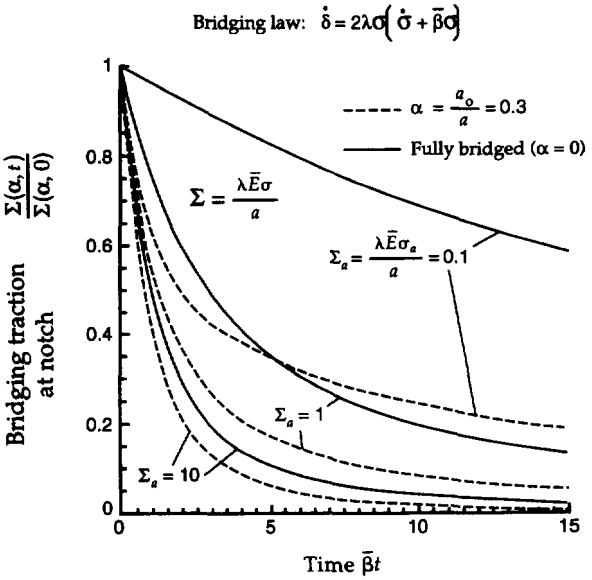

Fig. 6. Bridging stress at the notch (or center for the crack) for the case for three loads; $\Sigma_a = 0.1$, 1, 10.

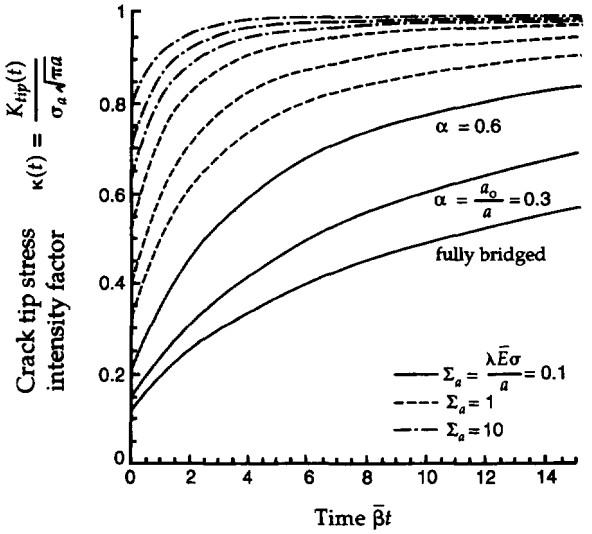

Fig. 7. Crack tip stress intensity factor as a function of time, for three loads and three notch sizes; $\Sigma_a = 0.1, 1, 10$; $\alpha = 0, 0.3, 0.6$.

6. DISCUSSION

Sections 4 and 5 compare the effect of two different simplifications; the effect of neglecting the convolution integrals was considered independently from the effect of approximating the spatial distribution of the bridging traction profile. Clearly, the bridging law (i.e., the convolution integrals) will affect the resultant bridging traction profile. However, considering high loads (or short cracks) minimizes the interplay between the two effects; for these cases, the crack opening profile (and thus the bridging tractions) is dominated by the near tip behavior of the bridged crack. As such, the comments made earlier concerning when it was appropriate to neglect the convolution integrals are still valid. Detailed computations are required to determine the combined effect at intermediate values of applied load or crack length.

It should be pointed out that crack growth problems, where new fibers are continually entering the wake of the crack, will behave very differently. As new fibers enter the crack, they respond elastically; the near-tip behavior can therefore be thought of as dominated

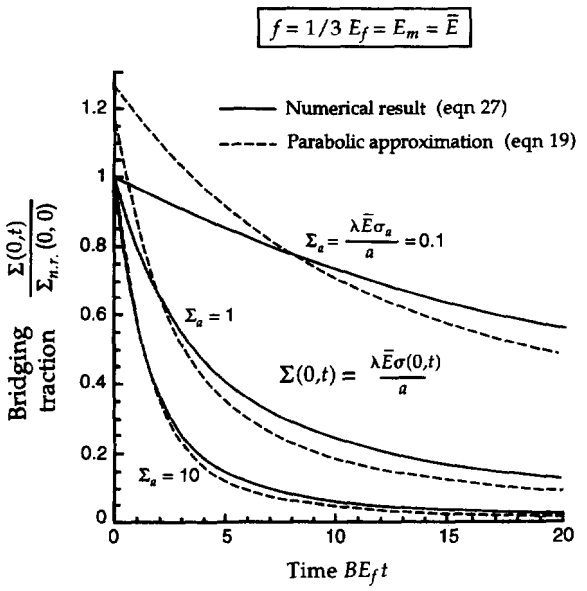

Fig. 8. Comparison of the bridging stress at the center of the crack predicted by parabolic approximation and full bridging calculations ($\Sigma_{n.r.}$ is bridging stress from full numerical calculations).

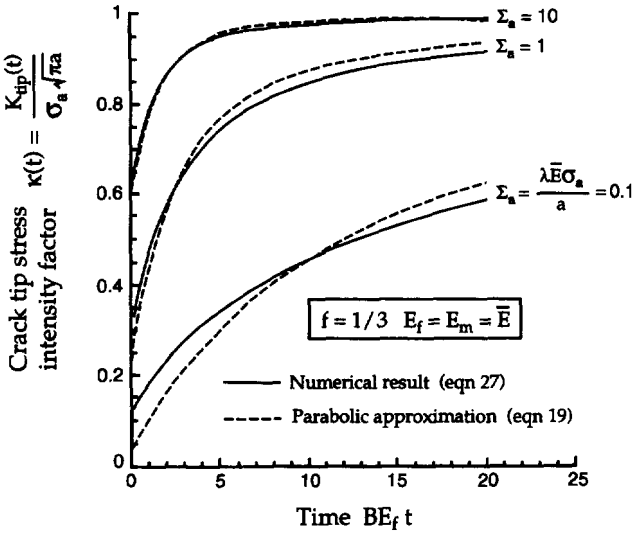

Fig. 9. Comparison of crack tip stress intensity factors predicted by the parabolic approximation and full bridging calculations ($\Sigma_{n.r.}$ is bridging stress from full numerical calculations).

by the short time response of the cell model. Hence, neglect of the convolution integrals is even more appropriate for crack growth problems.

It should be kept in mind that the solutions presented here neglect the possibility of a change in the direction of the shear stress in the sliding zone. If the strain rate in the matrix changes sign, the relative velocity between the matrix and fiber may change sign as well. This *must* be accompanied by a change in sign of the interfacial sliding stress. It is important to note that decreasing bridging tractions alone are a necessary but *not sufficient* condition for reverse slip to occur. The strain rate in the matrix will be comprised of two terms; the negative strain rate resulting from unloading of the unit cell and the positive strain rate due to fibers shedding load to the matrix. Only when the sum of these two terms is negative will the strain rate in the matrix be negative.

The models presented here neglect the possibility of a negative strain rate in the matrix. Such a situation, referred to as "reverse slip", is much more cumbersome to analyze when creep is present than it is for the rate-independent case. If fibers are creeping, the length of the "forward slip" zone is no longer necessarily constant, and the possibility exists that

both forward and reverse slip zones are time-dependent. A time-dependent bridging law which accounts for this is currently under development.

For stationary cracks, reverse slip zones would be more prevalent as the entire bridged region of the crack is unloading. In crack growth problems, however, the fibers near the tip region of the crack experience sharp increases in stress, decreasing the likelihood of reverse slip in this region. Since the near tip region has a dominant effect on crack velocity, it is reasonable to speculate reverse slip will not alter crack growth studies significantly.

7. SUMMARY

The time-dependent behavior of stationary cracks is shown to be well approximated by an appropriate assumed form of the bridging traction profile for very short cracks and high applied loads. For these cases, the simplification of an assumed profile allows the time dependence of the bridging stress profile to be captured in a single term. The relative effect of various approximations to a rather complicated bridging law can therefore be investigated in an efficient manner. The results show that the history dependence of the crack opening rate can be reasonably neglected at short times and for higher loads. With this in mind, full solutions for the bridging stress profile evolution were calculated using a simplified bridging law. The bridging stress profile evolution can be translated into evolution of the crack tip stress intensity factor. These results can be used in a straight-forward manner to predict initiation times for bridged cracks in ceramic matrix composites with creeping fibers.

Acknowledgements—This work was sponsored by the Advanced Research Projects Agency through the University Research Initiative at the University of California, Santa Barbara, ONR Contract N-0014-92-J-1808. A special thanks to Robert M. McMeeking for many helpful discussions.

REFERENCES

Bao, G. and McMeeking, R. M. (1994) Fatigue crack growth in fiber-reinforced metal matrix composites. *Acta Metallica et Materiala* **42,** 2415–2425.

Begley, M. R., Cox, B. N. and McMeeking, R. M. (1995a) Time dependent crack growth in ceramic matrix composites with creeping fibers. *Acta Metallica et Materiala* **43,** 3927–3936.

Begley, M. R., Cox, B. N. and McMeeking, R. M. (1995b) Creep crack growth and small-scale bridging in ceramic matrix composites. *Acta Metallica et Materiala* (submitted).

Begley, M. R., Evans, A. G. and McMeeking, R. M., (1995) Creep rupture in ceramic matrix composites with creeping fibers. *Journal of Mechanics and Physics of Solids* **43,** 727–740.

Begley, M. R. and McMeeking, R. M. (1995a) Fatigue crack growth with fiber failure in metal-matrix composites. *Composites Science Technology* **53,** 365–382.

Begley, M. R. and McMeeking, R. M. (1995b) Numerical analysis of fibre bridging and fatigue crack growth in metal-matrix composite materials. *Materials Science Engineering A* **A200,** 12–20.

Bourrat, X., Turner, K. S. and Evans, A. G. (1995) The microstructure of SiC/C composites and relationships with mechanical properties. *Journal of the American Ceramic Society* **78,** 3050–3056.

Cox, B. N. and Marshall, D. B. (1991) Stable and unstable solutions for bridged cracks in various specimens. *Acta Metallica et Materiala* **39,** 579–589.

DiCarlo, J. and Morscher, G. N. (1991) Creep and stress relaxation modeling of poly-crystalline ceramic fibers. In *Failure Mechanisms in High Temperature Composite Materials*, (eds G. K. Haritos *et al.*), ASME p. 15.

El-Azab, A. and Ghoniem, N. M. (1995) Investigation of incubation time for sub-critical crack propagation in SiC-SiC composites. *Journal of Nuclear Materials* **219,** 101–109.

Evans, A. G. and Zok, F. W. (1994) The physics and mechanics of fibre-reinforced brittle matrix composites. *Journal of Materials Science* **29,** 3857–3986.

Henager, C. H. and Jones, R. H. (1993) High temperature plasticity effects in bridged cracks and subcritical crack growth in ceramic matrix composites. *Materials Science Engineering-A* **166,** 211–220.

Henager, C. H. and Jones, R. H. (1994) Subcritical crack growth in CVI silicon carbide reinforced with Nicalon fibers: experiment and model. *Journal of the American Ceramic Society* **77,** 2381–2394.

Holmes, J. W. and Chermand, J. L. (1993) Creep behavior of fiber-reinforced ceramic matrix composites. In *High Temperature Ceramic Matrix Composites*, (eds R. Naslain *et al.*), Woodhead, U.K., p. 633.

Hutchinson, J. W. and Jensen, X. (1990) Models of fiber debonding and pull-out in brittle composites with friction. *Mechanics of Materials* **9,** 139–163.

Knauss, W. G. (1993) Time dependent fracture and cohesive zones. *Journal of Engineering Materials Technology* **115,** 262–267.

Marshall, D. B., Cox, B. N. and Evans, A. G. (1985) The mechanics of matrix cracking in brittle matrix fiber composites. *Acta Metallica et Materiala* **33,** 2013–2021.

McCartney, L. N. (1987) Mechanics of matrix cracking in brittle matrix fibre-reinforced composites. *Proceedings of the Royal Society of London* **A409,** 329–350.

McLean, M. (1985) Creep deformation of metal matrix composites. *Composites Science Technology* **23,** 37–52.
McMeeking, R. M. and Evans, A. G. (1990) Matrix fatigue cracking in fiber composites. *Mechanics of Materials* **9,** 217–227.
Schapery, R. A. (1975) A theory of crack initiation and growth in viscoelastic media : I. theoretical development. *International Journal of Fracture* **11,** 141–159.
Nair, S. V., Jakus, K. and Lardner, T. J. (1991) The mechanics of matrix cracking in fiber reinforced ceramic composites containing a viscous interface. *Mechanics of Materials* **12,** 229–244.
Tada, H., Paris, P. C. and Irwin, G. R. (1985) *The Stress Analysis of Cracks Handbook*, Del Research, St. Louis, MO.
Tressler, R. E. and DiCarlo, J. (1993) High temperature mechanical properties of advanced ceramic fibers. In *High Temperature Ceramic Matrix Composites*, (eds R. Naslain *et al.*), Woodhead, U.K., p. 33.

APPENDIX

The initial bridging stress profile at $t = 0$ is determined by solving the non-linear integral equation that results from the rate-independent analysis (Marshall *et al.*, 1985; McCartney, 1987; McMeeking and Evans, 1990; Cox and Marshall, 1991; Bao and McMeeking, 1994; Begley and McMeeking, 1995a; Begley and McMeeking, 1995b) For a center crack under remote tension, the governing equation for the initial traction profile is

$$\frac{[\Sigma(x)]^2}{4} + \int_x^1 \Sigma(\bar{x}) H(\bar{x}, x, 1)\, \mathrm{d}\bar{x} = \Sigma_a \sqrt{1-x^2}$$

where $\Sigma_a = \lambda \bar{E} \sigma_a / a$ is the normalized applied load.

The integral equations for the bridging tractions and their derivatives can be solved using the standard discretization technique summarized in [Begley and McMeeking, 1995b]. The result is a linear matrix equation for the bridging stress rate and a quadratic matrix equation for the initial condition. The differential equation given as (27) was integrated using a simple forward Euler method.

The fact that the crack is stationary greatly reduces the complexity of the problem; since the crack length is not changing, the coefficient matrix of the linear matrix equation (resulting from discretization of (27)) is the same for each time step. Once the coefficient matrix is filled in the usual manner, the vast majority of computational time is completed once and for all, and the solution proceeds quite rapidly. It is for this reason that a simple time integration scheme such as the forward Euler method used here is acceptable. Quick evaluation of the time derivatives means very small time steps can be taken without much penalty in computation time, insuring accuracy.